

7.6 Instrumentation for Vibration-Measurements

Every theoretical description has to face up to an evaluation via practical application. Of course, an equation representing a vibration will never completely cover the motion of a real string – but it does not have to, either, because that would make everything infinitely complicated. Rather, mathematics offer theoretical models, and it is the job of practical application to recognize the limitations of these models. The following chapters are to assist, and avoid that this practical evaluation does not itself become a source of uncertainty.

7.6.1 Impedance- / admittance-measurements

The mechanical impedance $\underline{Z} = \underline{F} / \underline{v}$ is calculated as the quotient of force and particle-velocity; the admittance is the reciprocal. The impedance-head is a typical sensor for measuring the impedance; in the case of the B&K 8001 we have a thimble-sized cylinder that contains, in its interior, two piezo-crystals. These crystals measure force and acceleration, with the latter yielding the velocity via integration over time. Now, any measurement will affect the value to be measured: sometimes almost not at all (for example radiation pressure in contact-free laser measurements), but sometimes significantly, as it happens e.g. in impedance measurements. This is due to the fact that the force sensor is not located directly at the measuring point but *within* the impedance head. From the force sensor, the connection to the external world is made via a rubber-cushioned nut. Since there is no mass-free nut, about 1 g of parasitic mass m_0 needs to be considered. If measurements at higher frequencies are the objective, further artifacts join the list. **Fig. 7.49** shows a measurement with the impedance head in the no-load condition:

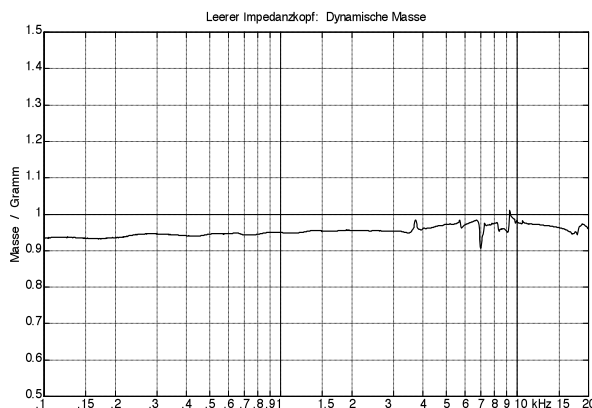
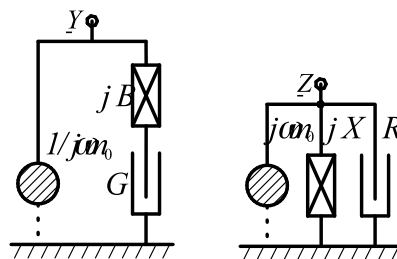


Fig. 7.49: Left: magnitude of the co-vibrating complex mass $\underline{F}/\underline{q}$ of the impedance head. Below: Force-flow-diagram of the equivalent systems. “Leerer Impedanzkopf” = impedance head by itself; “Dynamische Masse” = dynamic mass.



Depicted is the magnitude of the complex mass of just shy of 1 g. A tracer pin screwed into the nut increases the mass further so that in total 1.3 g of parasitic mass show up. This mass appears to act *ahead* of the measuring object (between impedance head and measuring object). In the force-flow-diagram, m_0 is connected in parallel to the device under test, because the flow-quantity force [3] is divided into two paths: the inertia-force for m_0 , and the force \underline{F}_M towards the measuring object: $\underline{F} = \underline{q} \cdot m_0 + \underline{F}_M$. The impedance \underline{Z}_M of the device under test is increased that way: $\underline{Z} = \underline{Z}_M + j\omega m_0$. The manufacturer is aware of this issue and therefore offers the **mass-compensation-unit** B&K 5565. Using the latter is not without its pitfalls, but we shall not go into more detail here: from today’s point-of-view, the 5565 is outdated. Also, the whimsicalities of polarity (the B&K 2625 inverts, the B&K 2623 does not) shall be mentioned here only in passing in this one sentence, although its disregard can cost you half your leave days ...

In Chapter 6, an up-to-date variant of the mass-compensation has already been introduced, and therefore we will look here merely at the effects of an uncompensated parasitic mass. Dividing the **impedance** Z into its real part R and its imaginary part X , we see that ωm_0 merely increases the reactance X . Therefore, if only the resistance R is of interest, we can do entirely without any mass compensation. For the **admittance** \underline{Y} , however, ωm_0 has effects on the susceptance B and the conductance G :

$$\underline{Y} = \frac{1}{1/\underline{Y}_M + j\omega m_0} = \frac{G + jB}{(1 - \omega m_0 B) + j\omega m_0 G} = \frac{G + jB(1 - \omega m_0 B)}{(1 - \omega m_0 B)^2 + (\omega m_0 G)^2}; \text{ with } \underline{Y}_M = G + jB.$$

The conductance $G = \text{Re}(\underline{Y}_M)$ of the device under test becomes a complicated term that corresponds to G merely in exceptional cases, and even then only in approximation (denominator $\rightarrow 1$). Generally, the discrepancy continues to decrease the smaller the parasitic mass m_0 is, and the lower the frequency becomes. **Fig. 7.50** shows the effects a 2-g-mass has on the calculation of conductance. Since it is difficult to predict how large the measurement errors will become without mass compensation, it is preferable to measure admittances generally only with mass-compensation.

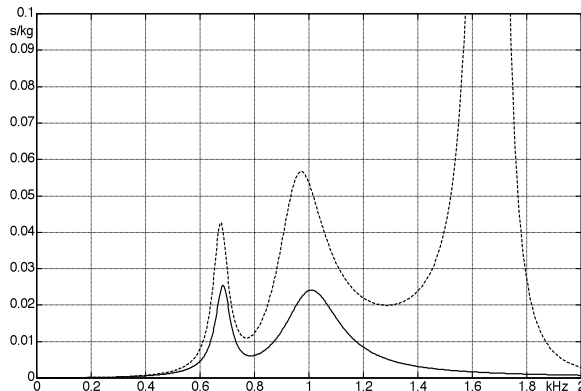


Fig. 7.50: Conductance without (—) and with (----) 2 g parasitic additional mass. At 1.7 kHz, the interaction of bearing suspension and additional mass results in an additional resonance peak.

For all analyses presented here, the force- and acceleration-signals of the impedance head were recorded using a Cortex CF-100 workstation; the mass-compensation was calculated using a Hilbert-transform. The typical noise-spectrum of the setup is shown in **Fig. 7.51**: clearly the **intrinsic noise** is negligible compared to the noise generated by the sensor. With 400 mV/N and 35 mV/g, the impedance head we used was sufficiently sensitive to capture small signals, as well – a dynamic-optimization adapted to the respective problem was nevertheless required for the corresponding measurements.

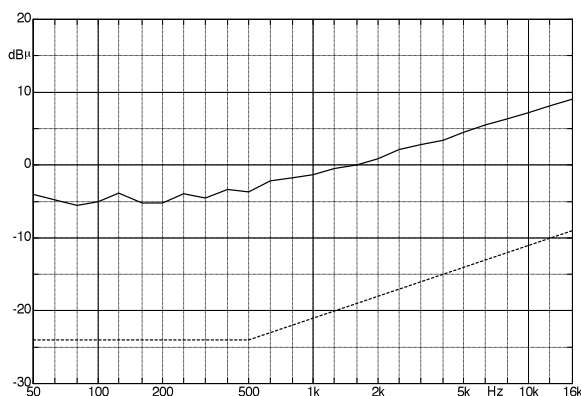


Fig. 7.51: 1/3rd-oct. analysis of the system noise: impedance head with charge amplifier (—); analyzer Cortex CF-100 (----). 0 dB μ \leftrightarrow 1 μ V.

Optimizing dynamics means adapting the dynamic range of the signal to the dynamic range of the system: on one hand we prevent weak signals from disappearing into noise while on the other hand avoiding overdrive in the signal paths. Usually, this works well for measurements taken at merely one frequency, but it may become an issue for broadband measurements. **Fig. 7.52** shows force and acceleration for the impedance head without load; both magnitudes change only by a factor of 1:20 across the frequency range – this is well manageable.

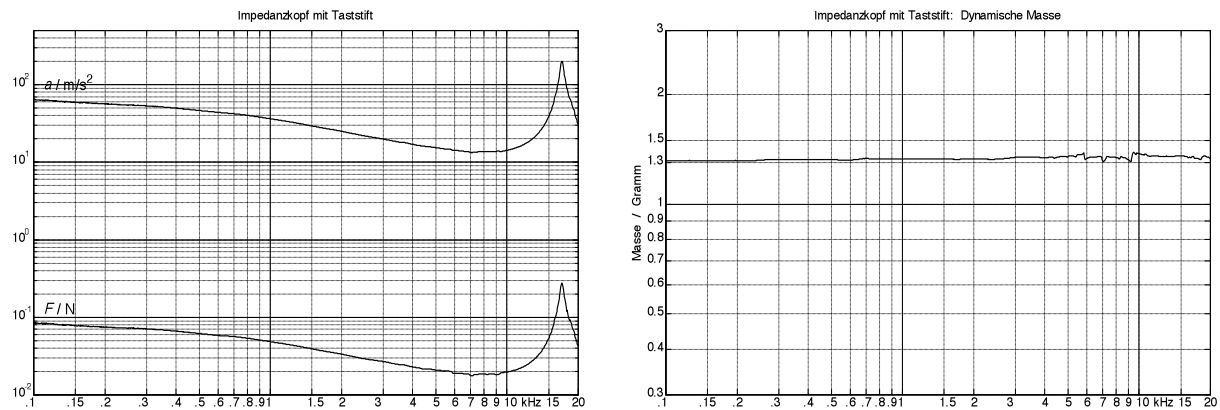


Fig. 7.52: Mechanical no-load condition: force and acceleration (left); dynamic mass (right); $U_{\text{Shaker}} = 2 V_{\text{eff}}$. “Impedanzkopf mit Taststift = impedance head including tracer pin; “Dynamische Masse” = dynamic mass

An impedance head in the no-load condition (open circuit, load impedance = 0) represents one extreme; the other extreme would be the firmly fixed head (short ckt, load imped. = ∞). The parasitic mass shows up for the open circuit, and the stiffness of the tracer pin can be seen for the short circuit – although only in approximation because a counter-bearing at complete rest is impossible to realize. To measure the stiffness, the tracer pin was set against a stone table of 200 kg; the result is shown in **Fig. 7.53**: we find a stiffness of $s = 6 \text{ MN/m}$ that – in conjunction with the parasitic mass (1.3 gram) – results in a resonance at 11 kHz. The force varied by a factor of 1000 in this measurement – given the dynamic range of the analyzer (100 dB), this should not be a problem. However, calculating the voltage generated by the sensor (400 mV/N) for a force of 1 mN, we arrive at merely 400 μV : for the broadband measurement, this is below the noise floor of the older charge amplifier (2625) used for this measurement. Still, the coherent averaging following the Hilbert transform manages to find a resonance at 11 kHz. The force minimum is not correctly identified in the broadband measurement, though: merely noise is detected (Fig. 7.53; selective meas'mnt \rightarrow Fig. 7.56a).

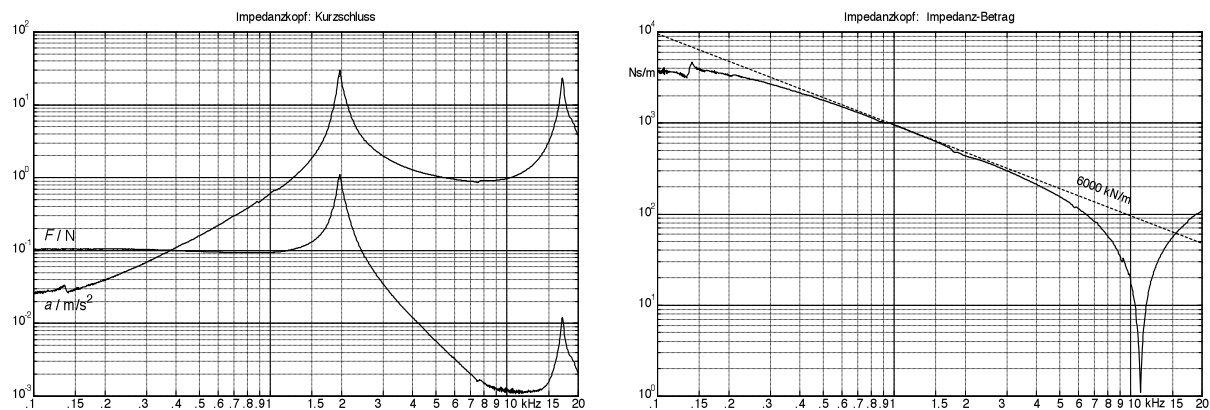


Abb. 7.53: Mechanical short circuit: force and acceleration (left, broadband), magnitude of the impedance (right, frequency-selective); $U_{\text{Shaker}} = 0,1 V_{\text{eff}}$. “Impedanzkopf” = impedance head; “Kurzschluss” = short circuit; “Impedanz-Betrag” = magnitude of impedance

It is difficult to foresee from which level of excitation-amplitude a structure will generate significant **non-linearities**. In any case, the drive-level limit given in the datasheet of the shaker must never be taken as a guide value for linear behavior. The maximum admissible supply voltage of $7 V_{\text{eff}}$ (B&K 4810) is a thermal limit that would have led to completely useless results of the present measurements. Even at merely $0,25 V_{\text{eff}}$, pronounced non-linearities showed up in the vicinity of the 1.9-kHz-peak, and only at $0.1 V_{\text{eff}}$ the nonlinear distortion was sufficiently small – but now the noise was too strong. This led to the question which control signal would be optimal.

The two classical excitation signals for measurements of the frequency response are sweep and pseudo-noise. For the **sweep**, the frequency of a sine tone increases over time, with the amplitude remaining constant. **Pseudo noise** is a special noise repeating after a period T . The density spectrum of the pseudo noise is constant (white), and its periodicity corresponds to the block length of the DFT-analysis (e.g. at 48 kHz sampling rate and $N = 4096 \Rightarrow T = 85,3 \text{ ms}$). Due to the strong time-variance of the short-term spectrum, time-weighting windows have to (!) be dispensed with – however, this does not pose any disadvantage because due to the identical periodicity there is no leakage. Also suitable is true stochastic noise (normal- or equal-distributed); however, this signal requires windowing and averaging.

Fundamentally, the frequency response of signal- and system-quantities may be explored via three different approaches: first, selective excitation and broadband measurement; second, broadband excitation and selective measurement, and third, selective excitation and selective measurement. Your typical sweep-measurement belongs to the first group, your typical noise-excitation to the second. Both approaches have disadvantages in case the system shows substantial non-linearities. A broadband measurement with sweep excitation may preclude capturing selective minima, as seen around 11 kHz for the force measurement in Fig. 7.53. Here, excitation via noise paired with selective analysis will deliver better results – but it may lead to arriving at the wrong conclusions in case of distortions: any signal limiting occurring at 1 kHz will change the results of the analysis at other frequencies. As a example, an arctan-function is inserted as a **non-linearity** into a band-pass system: the transfer function determined via DFT is bent more and more with increasing distortion – however, this happens not predominantly at 1 kHz, but at 3 kHz (k_3) and at low frequencies (difference tones). If this non-linearity would be connected in the signal flow ahead of the band pass, the measurement results would be useless – in their entirety, even.

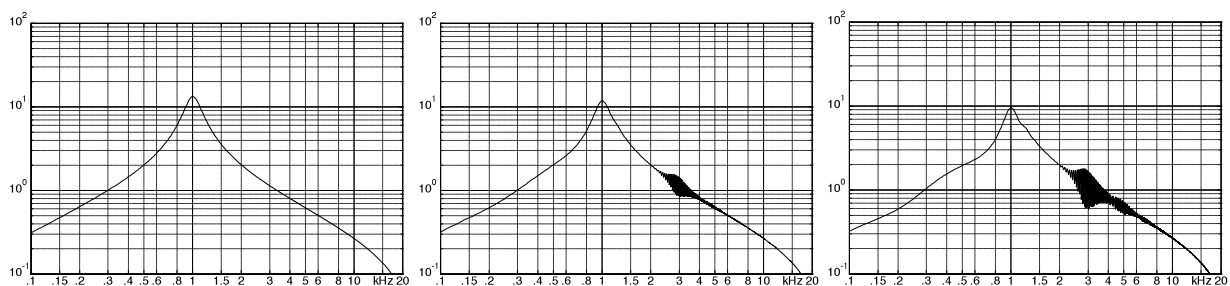


Fig. 7.54: System analysis with pseudo-noise and DFT: no/weak/strong non-linearity (left to right).

If mechanical systems are to be analyzed across several frequency decades, the measured quantity may vary by 10^5 ; a harmonic distortion of a “mere” 0.1% will become a serious issue here. The analyzer may have a harmonic distortion of 0.001% but the sensor is not likely to be up to this. Moreover, the distortion in the actor may even exceed 1%.

If limiting is introduced to the **sweep-sine-signal** by an arctan-function (non-linearity ahead of the system resonance), we get a different result: for frequencies around 333 Hz, the resonance amplifies the 3rd harmonic that is created by the non-linearity, while the higher frequency range is void of any selective errors (**Fig. 7.55**). If the non-linear limiting happens *post-system-resonance*, there is a tendency to represent the maxima with too small a value.

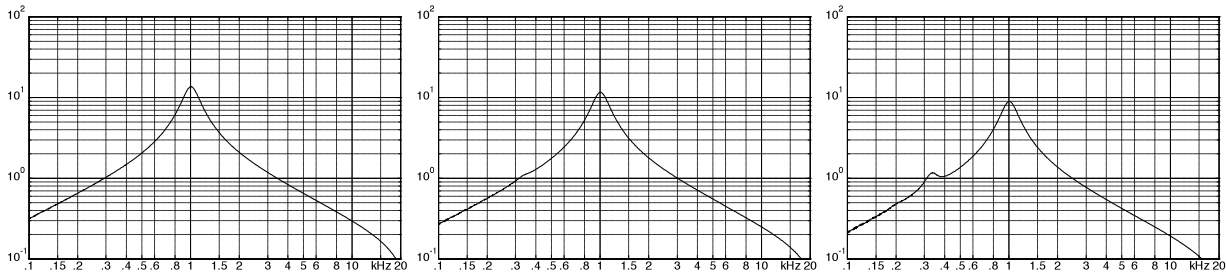


Fig. 7.55: System analysis using sweep: no/weak/stronger non-linearity *ahead* of the resonance (left to right).

The sweep measurement is least sensitive to non-linearities if the output signal of the system to be measured is filtered with a narrow-band **tracking filter** (selective excitation, selective measurement). For particularly pronounced signal dynamics, the frequency dependence of the sweep amplitude may additionally be matched to the system. Of course, corresponding filtering is possible for pseudo-noise, as well, since the periodicity does not change due to this. **Fig. 7.56a** compares sweep measurements with and without tracking filter – the result speaks for itself.

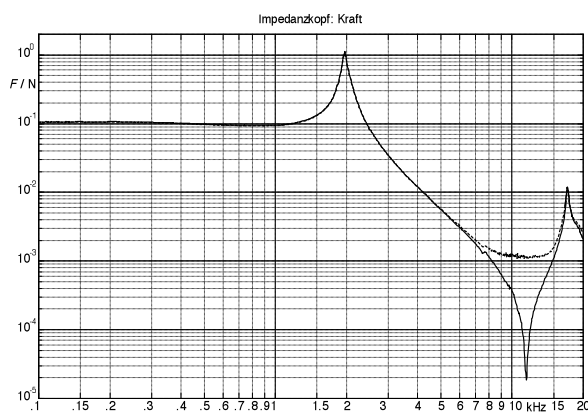


Fig. 7.56a: Force measurement; probe tip directed against the stone table. Without (----) and with (—) tracking filter. The force changes by 1:70000 across the frequency range; such a large dynamic range is only manageable with a selective measurement.
“Impedanzkopf” = impedance head, “Kraft” = force

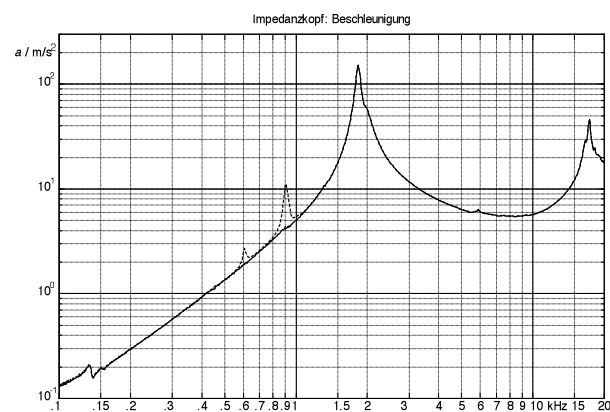


Fig. 7.56 b: Acceleration measurement, as given in Fig. 7.6.8a. Without (----) and with (—) tracking filter. At 600Hz and 900Hz, non-linearities excite the 1800-Hz-resonance.
“Impedanzkopf” = impedance head;
“Beschleunigung” = acceleration

During mechanical impedance measurements, interruptions in the force flux are a particular problem. The probe pin of the shaker cannot be welded to the guitar bridge (or fret) but it is pressed to the object using a constant **load offset**. For the B&K 4810, the largest admissible force is about 6 N. In this situation the shaker is already deflected to its limit, though, operating with strong non-linearity. A 3-N-offset would be the optimal theoretical value, with an alternating force of at the most 2 N_{eff} superimposed. Reducing the offset carries the risk that the probe pin lifts off, while increasing the offset will generate single sided force limitations (i.e. non-linearities). Sometimes there is the possibility to generate a load offset via supplementary spring; the force of this spring should not be included in the measurement.

7.6.2 The spectrum of decaying partials

An ideal, un-damped vibration of a string has a harmonic **spectrum** and may be represented by a Fourier-series without much effort. In a **real string**, however, several damping mechanisms are at work at the same time: the string itself radiates sound, heat is generated in its interior, and in the bearings, active power is withdrawn from the vibration of the string. The amplitudes of the partials (constants in the Fourier-series) become time-dependent, and the string vibration loses its periodicity. The standard tool for analyzing non-periodic vibrations is the **Fourier integral** comprising a special window-weighting. Choosing the parameters of the analysis, though, we run into the classic conflict of goals that cannot always be resolved satisfactorily: using a short window duration, the leakage effect broadens the frequency lines, but a long window duration will deteriorate the time resolution too much. If all partials were regularly spread out (Chapter 1.3), we would possibly be able to find an acceptable compromise, but the allpass-driven generation of additional tones requires an analysis with bands as narrow as possible (compare to Fig. 7.39).

As its amplitude becomes time-variant, the spectral line of a continuous tone (represented as a Dirac in the density spectrum) turns into an infinitely broad, continuous spectrum [6]. For the exponential decay process, the Dirac line needs to be convolved with the Fourier-transform of the e -function; the parameter of the latter is the **time constant** τ .

$$u(t) = e^{-t/\tau} \cdot \cos(\omega_0 t);$$

$$\underline{U}(j\omega) = (j\omega + 1/\tau) / [(j\omega + 1/\tau)^2 + \omega_0^2]$$

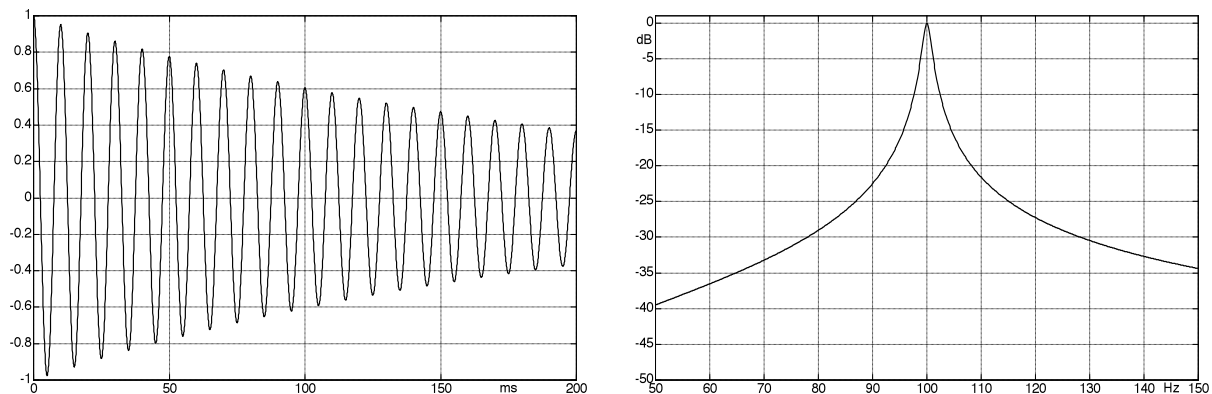


Fig. 7.57: Time function and spectrum of an exponentially decaying cosine-tone; $f = 100$ Hz, $\tau = 200$ ms.

The faster the tone decays (i.e. the smaller τ is), the broader the spectrum will be in the relevant level range. **Fig. 7.57** depicts time function and spectrum of a decaying 100-Hz-tone. In support of a purposeful presentation, the time constant is – at 200 ms – chosen to be relatively short; in guitar strings, values of in excess of 5 s are possible. The widening of the spectrum in Fig. 5.57 must not be confused with your typical DFT-leakage; rather, it results purely from the decrease of the amplitude over time. If we cut a DFT-**frame** (block) starting at $t = 0$ from the infinitely long time function, and transform it into the spectral domain (short-term spectrum), this weighing over time results in an additional convolution in the frequency domain. This is the **leakage** – an additional diffidence of the spectrum particularly noticeable in the area of the peak. The shorter the DFT-frame, the stronger the spectral diffidence is – with the shape of the weighing function over time (window function) to be considered as a further parameter.